



## Study of water sorption on modified Agave fibres

A. Bessadok<sup>a,b</sup>, D. Langevin<sup>a,\*</sup>, F. Gouanvé<sup>a</sup>, C. Chappey<sup>a</sup>, S. Roudesli<sup>b</sup>, S. Marais<sup>a</sup>

<sup>a</sup> Laboratoire "Polymères, Biopolymères, Surfaces", FRE 3101 Université de Rouen/CNRS, UFR des Sciences, 76821 Mont-Saint-Aignan Cedex, France

<sup>b</sup> Laboratoire de Polymères, Biopolymères, Matériaux Organiques, Faculté des Sciences de Monastir, Boulevard de l'Environnement 50019, Tunisia

### ARTICLE INFO

#### Article history:

Received 1 February 2008

Received in revised form 25 June 2008

Accepted 24 September 2008

Available online 10 October 2008

#### Keywords:

Natural fibres

Agave fibres

Water vapour sorption

Lignocellulosic

Chemical modification

Cell-wall structure

### ABSTRACT

Polymer composite materials are usually reinforced by synthetic matter such as carbon or glass fibres. However, owing to their good mechanical properties and low density, natural fibres are now increasingly being considered as reinforcement. With the aim of a new natural fibre based composite, various chemical treatments have been performed on Agave (*Americana* L.) fibres in order to improve their compatibility with the polymer matrix and to reduce their affinity for water. The effect of these treatments on the fibre water sorption power has been investigated by means of a micro-balance. Equilibrium water sorption isotherms have been deduced from weight variations of the fibres under water vapor pressure increments. Several specific physico-chemical models have been tested to describe the water sorption isotherms. The Park's model was found to describe the experimental results accurately and over a wide activity range. The sorption kinetics was also exploited in order to evaluate the diffusivity of water in the fibres. The variation of the water diffusion coefficient with water concentration is in agreement with the triple sorption mode described by the Park's model. These results show a global increase of moisture resistance of the fibres after chemical treatment. This effect is interpreted in terms of chemical and structural modifications of the cell-wall structure.

© 2008 Elsevier Ltd. All rights reserved.

### 1. Introduction

Historically many cereal straws have been used as raw materials for paper production (Atchison, Mc Govern, Kocurek, & Steven, 1983). These raw materials have gradually been replaced by wood products; nevertheless about 10% of the world overall pulp production is obtained from non-wood raw materials (Thykeson, Sjöberg, & Ahlgren, 1997). The main interest in pulp made from straw is that it provides excellent fibres for making paper with special properties, and that it is the major available source of fibrous raw material in some geographical areas. This is the case in Tunisia, which uses Alfa grass and Agave plants as main sources of fibres, in conjunction with the new eucalyptus wood resource (Ahrens, Gulya, Worry, & Walter, 1998; Anon, 1974). Agave (*Americana* L.) is a low growing, thick, long-leaved, subtropical plant used for commercial (rope, fibres, mescal and tequila), ornamental (yucca, century plant and mother-in-law's tongue), and medicinal (steroid extraction and pre-Columbian antibacterial salves) applications (Ricks, Vogel, Elston, & Hivnor, 1999).

The use of natural fibres in a thermoplastic matrix is highly beneficial because the strength and toughness of the resulting composites are greater than those of the unreinforced materials. Moreover, linocellulosic natural fibres are usually strong, light in weight (low density), cheap, abundant and renewable. Over the

past decade natural fibres have found use as a potential resource for making low-cost composite materials (Joseph, Thomas, & Pavithran, 1995).

One difficulty that has prevented the use of natural fibres is the lack of good adhesion with the polymeric matrix. In particular, the large moisture sorption of natural fibres adversely affects adhesion with hydrophobic matrix material leading to premature ageing by degradation and loss of strength. To prevent this phenomenon, fibre surface properties have been modified in order to promote adhesion (Khalil & Rozman, 2000). To reinforce thermoplastic composites, blue agave fibres were modified via the esterification reaction (Tronc et al., 2007). The mechanical properties characterization of these fibres showed a change in the elastic modulus and an improvement in the impact resistance.

In this paper, in order to both increase the moisture resistance of the reinforcing Agave (*Americana* L.) fibres and improve their adhesion with an unsaturated polyester matrix, different chemical surface treatments, previously applied by several authors to other fibres, have been carried out by using reagents such as acetic anhydride (Ac) (Khalil, Ismail, Rozman, & Ahmad, 2001), styrene (S) (Abdelmoula et al., 1997), acrylic acid (AA) (Khalil & Rozman, 2000) and maleic anhydride (MA) (Cantero, Arbelaiz, Llano-Ponte, & Mondragon, 2003).

The aim of the present work is principally to investigate the natural fibre behaviour towards water molecules by means of microgravimetric measurements. The effects of treatments have been analysed from spectroscopic and microscopic surface analysis,

\* Corresponding author. Tel.: +33 02 35146707; fax: +33 0235146704.

E-mail address: [dominique.langevin@univ-rouen.fr](mailto:dominique.langevin@univ-rouen.fr) (D. Langevin).

**Symbol list**

$a_w$	Water vapour activity	$N$	Number of groups in a fibre population
$A_L$	Specific sorption sites capacity	$p_{w, \text{ sat}}$	Saturated water vapour pressure
$B_L$	Affinity constant	$p_w$	Water vapour pressure
corr	Index for “corrected”	$r$	Fibre radius
$C_w$	Water concentration	$\langle r_{nb} \rangle$	Number-average radius
$C_m$	Concentration due to adsorbed water in a monolayer	$\langle r_w \rangle$	Weight-average radius
$D, D_1, D_2$	Diffusion coefficient of water, for short and long times sorption	$r_0$	Minimal fibre radius
eq	Index for “equilibrium”	$r_N$	Maximal fibre radius
exp	Index for “experimental”	$Q_t$	Water uptake at time $t$
$E$	Average deviation modulus	$t$	Time
$K_a$	Aggregation equilibrium constant	$t_d$	Time lag
$K_{ads}$	Constant linked to the adsorption energy of a layer	$\alpha$	Parameter in Eq. (6). (Dimensionless)
$M_d$	Mass of dry mater	$\rho$	Volumic mass
$M_w$	Mass of sorbed water at equilibrium	$\tau$	Dimensionless time ( $=D.t/r^2$ )
$n$	Mean number of water molecules in an aggregate	$\Delta m_t$	The mass of water sorbed at time $t$ during the sorption stage
$n_T$	Total number of fibres in a sample	$\Delta m_{eq}$	The mass of water sorbed at equilibrium

water sorption kinetics results and equilibrium water sorption isotherms. To interpret the sorption isotherms, different models from the literature have been tested.

## 2. Theoretical background

### 2.1. Water sorption models

When a sample of a material is placed in a humid atmosphere, the relationship between the ambient water activity  $a_w$  and the equilibrium sample sorbed water concentration  $C_w$ , at a given temperature, is described by an equilibrium sorption isotherm ( $C_w = f(a_w)$ ).  $C_w$  can be defined as the ratio of the mass of water sorbed at equilibrium ( $M_w$ ) to the mass of dry matter ( $M_d$ ):

$$C_w = \frac{M_w}{M_d} \quad (1)$$

Water activity ( $a_w$ ) at a given temperature is defined as the ratio of the water vapour pressure  $p_w$  to the saturated water vapour pressure  $p_{w, \text{ sat}}$ :

$$a_w = \frac{p_w}{p_{w, \text{ sat}}} \quad (2)$$

Sorption models, linking  $C_w$  and  $a_w$  (or  $C_w$  and  $p_w$ ), are useful for predicting water sorption properties of materials. Their adequacy with the experimental sorption results gives some informations concerning the sorption mechanism and possible interactions between the substrate and water (Leung, 1983). Many sorption models exist in the literature to describe water sorption in cellulosic materials (Aranberri-Askargorta, Lamptke, & Bismarck, 2003; Iglesias & Chirife, 1975; Toribio, Bellat, Nguyen, & Dupont, 2004).

The classification made by Rogers (1965) of gas and vapour sorption in polymer materials highlights five fundamental sorption modes: Henry, Langmuir, Dual-mode, Flory–Huggins and type IV. The type IV isotherms present a sigmoid shape which reflects a complex combination of several sorption modes; this is usually encountered with water sorption in hydrophilic polymers like ion-exchangers and natural materials, such as starch or flax fibres. Considering the complex and heterogeneous structure of the natural fibres, where cell-walls, dense material and porous domains coexist, sigmoid isotherms can be described by at least two kinds of model.

The adsorption models, such as BET and GAB models (Brunauer, Emmett, & Teller, 1938; Park, 1986) which consider that water

molecules condense layer by layer on adsorption surfaces (external surfaces of specific sites or internal surfaces of micro-pores/cavities for instance). These models need two quantities to be defined, the amount of water  $C_m$  corresponding to one monolayer and the constant  $K_{ads}$  linked to the adsorption enthalpy difference between the first layer and the following. For example BET model was used to determine the quantity of moisture adsorbed as a monomolecular layer on the surface of lyocell and cotton fibres (Okubayashi, Grissier, & Betchold, 2004). GAB model was used to fit cassava starch film sorption isotherm data (Mali, Sakanaka, Yamashita, & Grossmann, 2005).

The model of Park (Guggenheim, 1966) which assumes the association of three mechanisms: non-specific sorption (Henry's law, molecular solution in a rubbery polymer); specific sorption (Langmuir's mode), on special sites; and water molecule aggregation (clustering) at high water activity. The specific sites of sorption can be ions, polar groups, micro-cavities or micro-porosities, and are often considered as the nuclei of the water aggregates. As suggested by Morton et al. water molecules adsorb directly on cellulose hydroxyl groups of external surface, amorphous regions, inner surface of voids and crystallites. Additional water molecules can adsorb on the water molecules binding the fibre directly (Morton & Hearle, 1997). The model of Park [ $C_w = f(a_w)$ , Eq. (3)] comprises three terms. The first term describes Langmuir sorption which leads to a plateau of concentration when water activity increases, corresponding to the saturation of the specific sites of sorption. The second term gives a water concentration which increases linearly with water activity (Henry's law). And the third term is a power function which represents the aggregation phenomenon based on the equilibrium:  $n\text{H}_2\text{O} \xrightleftharpoons{K_a} (\text{H}_2\text{O})_n$ .

Park's model needs five parameters to be defined:  $A_L$ , the concentration of the specific sorption sites;  $B_L$ , the affinity constant of water for these sites;  $K_H$ , the constant of Henry's law;  $K_a$ , the equilibrium constant of aggregation and  $n$ , the mean size of the aggregates.

$$C_w = \frac{A_L \cdot B_L \cdot a_w}{1 + B_L \cdot a_w} + K_H \cdot a_w + K_a \cdot a_w^n \quad (3)$$

### 2.2. Sorption kinetics

A change of water vapour activity around the sample (from  $a_{wi}$  to  $a_{w(i+1)}$ ) induces its water content to change with time until a new equilibrium is reached. The analysis of these sorption (or

desorption) kinetics allows the diffusivity of water in the material to be calculated assuming some hypothesis. Kohler et al. have reported that water exchange on natural fibres such as flax and hemp can be modeled by two parallel independent first order processes, which was defined PEK (parallel exponential kinetics) model (Kohler, Dueck, Ausperger, & Alex, 2003). The model offered two different mechanisms for the exchange of water vapor relating to different sorption sites. According to their method, experimental data of the moisture content is simulated as a function of time using Eq. (4), where  $M_t$  and  $M_{inf}$  are the mass change at any time  $t$  and at equilibrium state.  $\tau$  is a characteristic time to obtain approximately 63% of  $M_{inf}$ .

$$M_t = M_{inf1} \cdot (1 - e^{-t/\tau_1}) + M_{inf2} \cdot (1 - e^{-t/\tau_2}) \quad (4)$$

Subscripts 1 and 2 indicate the two kinetic processes defined as fast and slow, corresponding to slow and fast sorption sites. The fast and slow sorption sites can be related to different types of amorphous regions, external/internal fibre surfaces and direct/indirect sorption (Morton & Hearle, 1997). The direct sorption of the water molecules onto the external surface and amorphous regions could be fast while the indirect sorption onto the inner surface and crystallites could be relatively slow.

In this work, Agave fibres are treated as dense and homogeneous cylinders while the transport phenomena are assumed to be governed by solution-diffusion mechanisms and described by models (Fick's laws) relative to the transport of small molecules in polymers.

Considering the usual initial and boundary conditions applied by Crank (1975), Crank and Park (1968) for gas and vapour sorption measurements, Fick's laws lead to the two following analytic solutions for a full cylinder of radius  $r$  ( $r < < \text{length}$ ):

$$Q_t = \frac{\Delta m_t}{\Delta m_{eq}} = \frac{4}{\sqrt{\pi}} \tau^{1/2} \left[ 1 - \frac{\sqrt{\pi}}{4} \tau^{1/2} - \frac{\tau}{12} \dots \right] \quad (5)$$

$$Q_t = 1 - \sum_{n=1}^{\infty} \frac{4}{\alpha_n^2} \exp(-\alpha_n^2 \tau) \quad (6)$$

Where  $\tau = D.t/r^2$  is the dimensionless time,  $D$  is the diffusion coefficient of water in the material and  $t$  is the time.

$Q_t$  is the sorption uptake;  $\Delta m_t$  is the mass of water sorbed at time  $t$  during the sorption stage and  $\Delta m_{eq}$  is the mass of water sorbed at equilibrium. The  $\alpha_n$  values correspond to the roots of the zero order Bessel function of the first kind (Angot, 1965).

### 3. Experimental

#### 3.1. Agave fibres

Agave fibres (*Americana* L.) were obtained after pre-treatment of the plant leaves. In a first step, pieces of leaf (10 g) were washed in 2 l of milli-Q® water for 24 h at 25 °C. These sheets were then immersed in a solution of pectinase [*Aspergillus aculeatus*] (5 ml for 1 l of milli-Q® water) for 12 h at 25 °C. In a second step, the fibrous bundles so obtained were washed with milli-Q® water and then whitened with a bleaching solution (10 ml H<sub>2</sub>O<sub>2</sub> in 1 l milli-Q® water) at ambient temperature until a neutral solution (pH 7) was obtained. After washing several times in water and acetone, the fibres were dried in an oven for 12 h at 60 °C and then placed in a desiccator under vacuum with P<sub>2</sub>O<sub>5</sub> at ambient temperature.

Like many natural fibres, Agave fibrous bundles are composed mainly of cellulose, lignin and hemicellulose (Cruz, Mendoza, Calado-Vieira, & Heinze, 1999; Iniguez-Covarrubias, Diaz-Teres, Sanjuan-Duenas, Anzaldo-Hernandez, & Rowell, 2001). Lignocellulosic structure is constituted by several layers concentrically arranged and with different compositions. Chains of cellulose, the main reinforcement material, form microfibrils which are held together by

amorphous hemicellulose and lignin and aggregates into longer microfibrils helically wound along the fibre axis and embedded into an amorphous lignin/hemicelluloses matrix (Tronc et al., 2007). The fibrils are assembled in several layers to build up the structure of the fibre. Fibres are cemented together in the plant by lignin, pectins, hemicelluloses which can be dissolved in alkaline conditions. Waxes due to fatty acids are also components of the fibre which can be found on the surface. Fig. 1 shows SEM photographs of fibre bundles. A schematic diagram of a lignocellulosic fibre structure is given in Fig. 2.

As they are natural products, the fibres are heterogeneous. From optical microscopy observations, the Agave fibres present a radius ranging from 50 ( $r_0$ ) to 170  $\mu\text{m}$  ( $r_N$ ) and a density  $\rho = 0.74 \text{ g/cm}^3$ .

As detailed in Appendix A, for a given sample of  $n_T$  fibres, one can define a number-average radius  $\langle r_{nb} \rangle$ ,

$$\langle r_{nb} \rangle = \sum_{i=1}^{n_T} r_i / n_T \quad (7)$$

which was found equal to 109.4  $\mu\text{m}$  for the untreated Agave fibres obtained.

It is also convenient to express a weight average radius, found equal to 122  $\mu\text{m}$ :

$$\langle r_w \rangle = \sum_{i=1}^N n_i r_{i,m}^3 h_i / \sum_{i=1}^N n_i r_{i,m}^2 h_i \quad (8)$$

Fig. 3 presents the histograms of the radius number (a) and weight (b) distributions of the fibres considering  $N = 12$  radius groups of width  $\Delta r = 10 \mu\text{m}$ .

#### 3.2. Chemical treatments and surface characterization

The Agave fibres obtained following the above protocol have been treated by maleic anhydride (MA), acetic anhydride (Ac), acrylic acid (AA) and styrene (S). The treatment protocol and the chemical reactions involved are the same as those presented in details in our previous paper relative to the chemical modification of Alfa fibres (Bessadok et al., 2007). As in this previous study, the effects of the chemical treatment on Agave fibres were observed by using SEM (CAMBRIDGE S200 SEM) and fluorescent microscopy (LEICA DM LM) after drying and treatment of the sample by a fluorescent probe (Calcofluor White M2R, CAS: 4404-43-7, 0.01% w/v). All the images were taken in the same operating conditions. FTIR (Nicolet AVATAR 360) in ATR mode was also used to characterize chemical changes induced by the treatment of the fibres.

#### 3.3. Water vapour sorption studies

Water uptake has been measured by using an electronic microbalance (IGA-002, supplied by Hiden Analytical, Warrington (UK)) in its "Humidifier" configuration. After transferring the sample (fibre bunch of about 20 mm in length and 100 mg in mass) to the measurement reactor, this is dried by circulating dry Nitrogen (200 cm<sup>3</sup>/min) until a constant weight is obtained. The sample environment temperature is controlled by a thermoregulated water bath.

Then water vapour pressure is increased in appropriate steps up to saturation vapour pressure by circulating a mixture of two gas [A, dry nitrogen; B, water saturated nitrogen] whose composition A/B is adjusted by the IGA software (overall flow = 200 cm<sup>3</sup>/min) in order to maintain the required humidity. At each step, the mass gain is measured as a function of time until an equilibrium state is reached. The water content at equilibrium is used to build the sorption isotherm. More details have been reported elsewhere (Detallante et al., 2002). In this work the water sorption measurements have been performed at 25 °C.

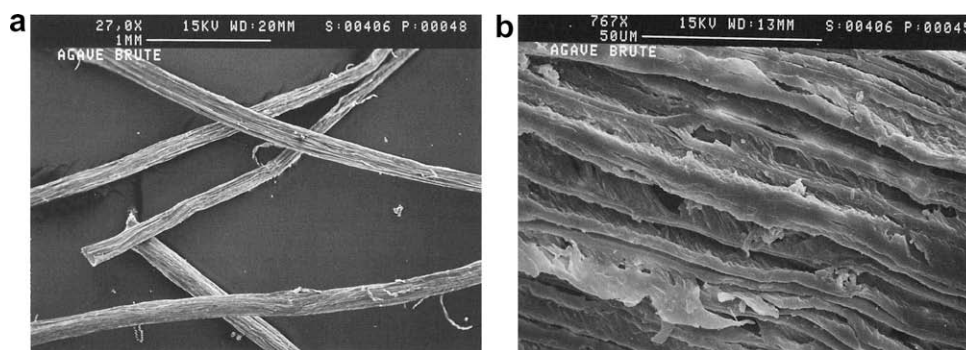


Fig. 1. (a, b) SEM photographs of Agave microfibril bundles. The scale is indicated on the views.

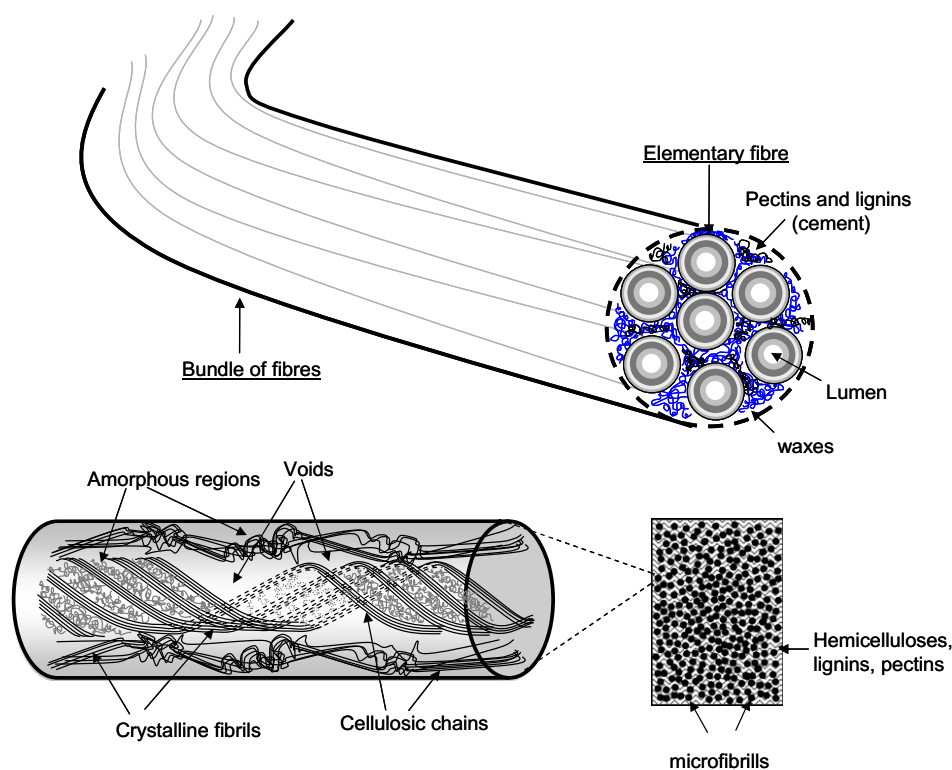


Fig. 2. A schematic diagram of a lignocellulosic fibre structure.

## 4. Results and discussion

### 4.1. Effects of the chemical treatments on the fibres

#### 4.1.1. IR spectroscopy analysis

The comparison of the IR spectra of Agave fibres before and after chemical treatment, presented in Fig. 4a–b, shows the chemical changes brought by the (MA), (Ac), (AA) and (S) reagents. The spectra were baseline corrected and normalized at  $1160\text{ cm}^{-1}$ , the major absorbance peak (C–C ring breathing) reflecting the carbohydrate backbone of cellulose (Bellamy, 1975; Garside & Wyeth, 2003; Grunert & Winter, 2000; Olson & Salmèn, 2004). These spectra present in common other peaks characteristic of the mainly cellulosic structure of the fibres: C–O–C glycosidic stretching at  $\sim 1100\text{ cm}^{-1}$ , C–OH stretching vibration at  $\sim 1060\text{--}1050\text{ cm}^{-1}$ , O–H deformation of alcohol groups at  $\sim 1360, 1320\text{ cm}^{-1}$ , OH and  $\text{CH}_2$  groups at  $\sim 3400$  and  $2920\text{ cm}^{-1}$ .

Due to the introduction of (CH) and ( $\text{CH}_2$ ) groups by styrene and acrylic acid, the spectra of the (S) and (AA) treated Agave fibres

present stronger bands at  $\sim 2960\text{ cm}^{-1}$ ,  $\sim 2900\text{ cm}^{-1}$  and  $\sim 2855\text{ cm}^{-1}$  than for the other fibres. At the same time the new ester groups resulting from the acidic (AM), (AC) and (AA) treatments are highlighted by the band at  $1730\text{ cm}^{-1}$  characteristic of the carbonyl (C=O) group. In the case of untreated and (S) treated fibres, the low intensity peak at this position indicates the presence of residual pectins which have not been eliminated by the preliminary pectinase treatment (cf. Section 3.1). Finally, the appearance in the (S) treated fibre spectrum of peaks at  $3025\text{ cm}^{-1}$ ,  $1500\text{ cm}^{-1}$ ,  $800\text{ cm}^{-1}$  and  $700\text{ cm}^{-1}$ , corresponding to the (CH) vibration in aromatic groups, indicates clearly the presence of polystyrene in the fibres.

#### 4.1.2. Microscopy

Fluorescent microscopic images in Fig. 5 show (several images) the rate of fixation of calcofluor by the untreated and treated fibres. Calcofluor is a fluorescent probe well known to have high affinity with polysaccharides such as cellulose which is visualized by dark blue patches at the surface of the fibres. The treated fibres are



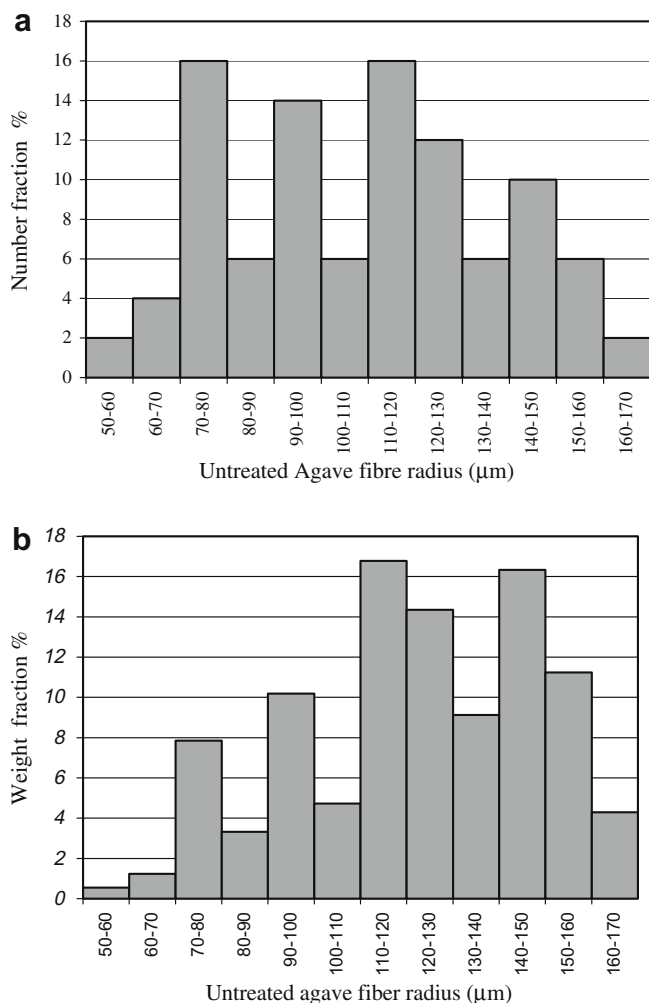


**Fig. 3.** Untreated Agave fibres: number (a) and weight (b) radius distribution, with  $r_0 = 50 \mu\text{m}$ ,  $r_N = 170 \mu\text{m}$ ,  $\langle r_{nb} \rangle = 109 \mu\text{m}$  and  $N = 12$  ( $\Delta r = 10 \mu\text{m}$ ).

clearly less coloured than the untreated one indicating that the treatments have inhibited access to the superficial cellulose of the fibres. Different mechanisms can be assumed for this inhibition: formation of ester groups by reaction with acid reagents (AA, AM, AC) but also changes of the fibre structure (density, roughness ...) associated with the elimination of pectic substances, lignin and the amorphous waxy cuticle. It emerges from these images that it is rather difficult to give a quantitative conclusion concerning the efficiency of the chemical treatments.

Comparing SEM images shown in Fig. 6 (treated fibres) with those in Fig. 1 (untreated fibres) it appears that the chemical treatments modify not only the chemical nature but also the superficial morphology of the fibres. The untreated Agave (Fig. 1) presents regular fibres showing amorphous cementing zones (waxes, fatty acids, gums, lignin ...) and some superficial spiral cellulose structures with few lignin residues. In Fig. 6, in the (a) series, a more or less marked fibre bursting is observed according to the treatment. This effect is weak with (AA) (3.a) and increases in the order (Ac) (4.a), (AM) (2.a) and (S) (1.a). Depending on the particular thermal and chemical treatment, the cellulose is more or less cleared out of the waxy cover and of the cements which bind the fibres together. Similar observations have been made about Sisal and Flax fibres (Bledzki & Gassan, 1999; Rong et al., 2001; Sreekala & Thomas, 2003; Kreze et al., 2005). In the (b) series, in addition to the spiral cellulose disorganization, it can be observed that (S)

treatment (1.b) induces the formation of nodules certainly due to polystyrene inclusion in the cementing material which loses partly its linking character and becomes less hydrophilic. After (AM) (2.b) and (AA) (3.b) treatments we can observe the alignment of the microfibrils which remain linked by a residual cement fraction.

The partial elimination of the cementing materials leads to the modification of the roughness and the chemical nature of the fibre surface. The treatments have effectively modified the surface of the microfibrils which appear more smooth or sleek than in the case of the untreated fibres.

#### 4.1.3. Effect of the treatment on the fibre radius

The microscopic observations reveal, in addition to the surface modifications, significant changes in the dimensions of the fibres subsequent to the partial elimination of the cementing material. Fig. 7 shows fibre radius distribution histograms assessed after treatment by the (S), (AA), (Ac) and (AM) reagents. These diagrams can be compared to Fig. 3 representing the same histogram for the initial untreated Agave fibres. In every case one can observe that the fibre radius decreases noticeably after treatment. The size of this effect is shown in Table 1 which gives the number-average radius  $\langle r_{nb} \rangle$  of the fibres before and after treatment and its reduction ratio. The change in dimension will be considered in the interpretation of the water vapour sorption experiments.

### 4.2. Water vapour sorption equilibrium

#### 4.2.1. Equilibrium sorption isotherms

The water vapour sorption experimental results plotted for the untreated Agave fibres are presented in Fig. 8. The isotherm presents a sigmoid or S-shape corresponding to type IV of the Rogers classification (Rogers, 1965). This is frequently observed in cellulose based materials (Jonquière and Fane, 1998) and can be generalized to many hydrophilic materials. Our aim in this paper is to analyse the sorption results in relation to the sorption models mentioned previously (cf. Section 2.1). BET, GAB and Park's models have been tested and compared. For more clarity, only the results obtained with the Park's model are commented. This model has been considered as the more relevant, in reference with its accuracy and the extent of its activity range application.

The hypotheses leading to the model of Park (Eq. (3)) are quite different from those advanced for GAB and BET models. Park's model assumes first that a fraction of water molecules can be adsorbed on specific sorption sites. This behaviour results from a combination of two processes: an adsorption at the surface of micro-cavities (free volume, micropores ...) and an adsorption due to the presence of hydrophilic groups (hydroxyl groups of cellulose). Such specific sites exist also at the periphery of the fibre bundles and consist of the negative charges of the galacturonic acid of the pectin-like molecules. It is also supposed that part of the water is absorbed non-specifically in amorphous fractions of the material, according to the Henry's mode of dissolution. This mode mainly operates in the matrix of the secondary wall of the fibres where pectic polyanions are also present. At the highest water activities ( $a_w > 0.5$ ), it is assumed that the sorbed water can cause swelling of the fibres and form aggregates of several molecules; this takes place in the heart of the elementary fibres, named the lumen, but also in the water free space corresponding to the macropores of the cell-walls.

From the shape of the experimental sorption isotherms it seems that the Langmuir sites are saturated beyond  $a_w \approx 0.1$  or  $0.2$  and that the formation of aggregates is negligible below  $a_w \approx 0.5$ . On this basis it is assumed that in the range  $0.1 < a_w < 0.5$  the sorption follows a linear law:

$$Y_1 = C_w = K_H a_w + A_L \quad (9)$$

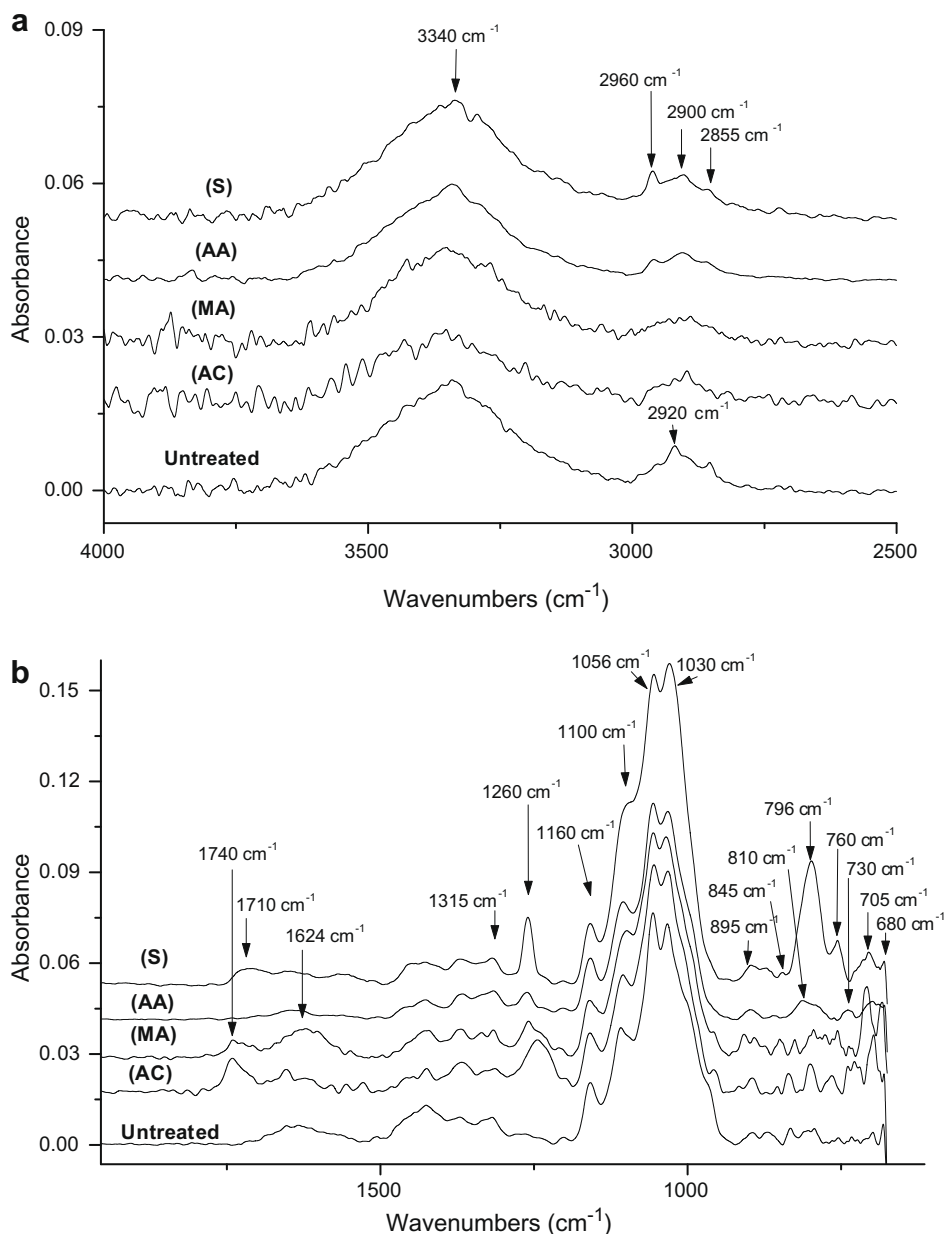


Fig. 4. FTIR spectra of untreated and treated Agave fibres.

By a linear regression using Eq. (9) one can calculate the Henry's constant  $K_H$  and the concentration  $A_L$  of the specific sites of sorption.

Afterwards, in the activity range where the aggregates predominate ( $0.5 < a_w < 0.9$ ), the function  $Y_2$  is calculated:

$$Y_2 = C_w - K_H a_w - A_L = K_a a_w^n \quad (10)$$

$K_a$  and  $n$  are then evaluated by linear regression of Eq. (10) rewritten as:

$$\text{Log} Y_2 = n \text{Log} a_w + \text{Log} K_a \quad (11)$$

It is possible to improve the fit by replacing  $Y_1$  (in Eq. (9)) with  $Y_3$ :

$$Y_3 = C_w - K_a a_w^n = K_H a_w + A_L \quad (12)$$

After two or three iterations, convergent values of  $A_L$ ,  $K_H$ ,  $n$  and  $K_a$  are obtained.

The calculated parameter values are presented in Table 2. In the present case, it was not possible to give a significative value

of the parameter  $B_L$ , because of the lack of numerous and precise experimental points for water activity inferior to 0.1. Fig. 8 compares the experimental points and the calculated curve according to Park's model in the activity range  $0.1 < a_w < 0.9$ , the deviation modulus  $E^1$  is found to be equal to 20% indicating a good fitting of the model.

Table 3 allows us to compare these results to the Park's parameters published previously for Alfa and Flax fibres (Bessadok et al., 2007; Gouanvé, Marais, Morvan, Métayer, & Poncin-Epaillard, 2006).

<sup>1</sup> The ability of a model to fit with the experimental points was evaluated thanks to the average deviation modulus  $E$ :

$$E = \frac{100}{N} \sum_{i=1}^N \frac{|m_i - m_{pi}|}{m_i}$$

where  $m_i$  is the experimental value,  $m_{pi}$  is the computed value and  $N$  is the number of experimental points. An  $E$  modulus inferior to 10% was taken to indicate a valid fitting.

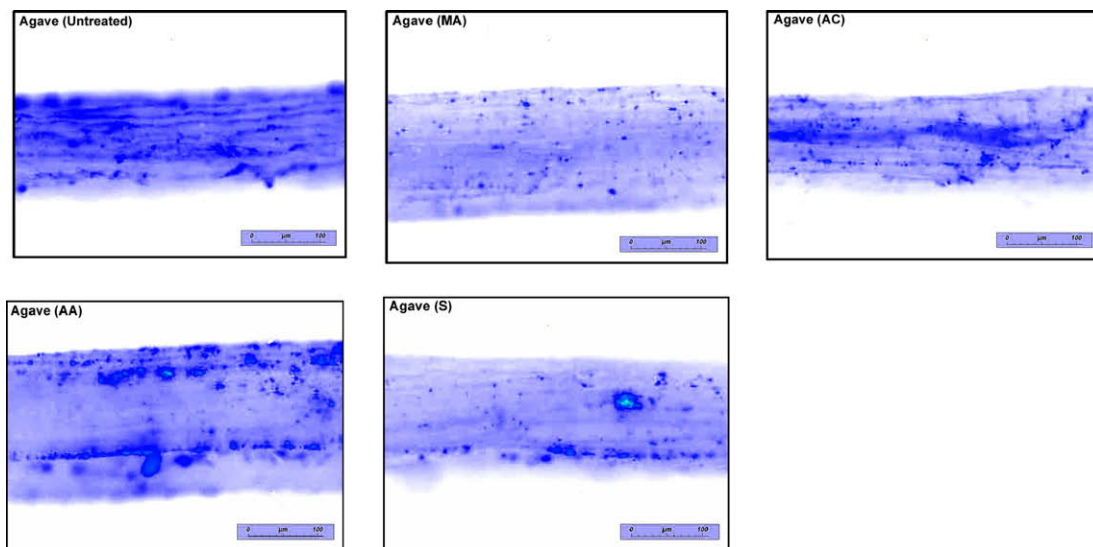


Fig. 5. Fluorescent microscopy images of untreated and treated Agave fibres.

#### 4.2.2. Models and real systems

The Agave fibres form a complex system containing a high proportion of cellulose bearing three hydrophilic groups ( $-\text{OH}$ ) per  $-\text{C}_5\text{H}_{10}\text{O}_5-$  unit. The calculated values of  $A_L$  (0.015 g water/g of cellulose), which should represent the content of hydrophilic groups able to retain water molecules, is well below those corresponding to three water molecules binding per cellulose motif (0.36 g water/g of cellulose). This could be explained by the experimental water sorption measurement method used. In the gravimetric measurements the sample is first kept under a dry nitrogen gas sweeping in order to remove water out of the sample. It is likely that some water molecules, strongly bound or hardly accessible, remain in the “dry” sample. This would result in an overestimation of the dry mass of the sample and a diminution of the number of accessible sites for new molecule sorption. In addition, the proposed models are phenomenological and give only a simplified representation of the real systems. Moreover, it should be noticed that the access of water molecules to cellulose can be reduced by the presence of strong interactions, such as hydrogen bonds, knowing that cellulosic structure is characterized by amorphous and crystalline zones in microfibril forms.

#### 4.2.3. Influence of the chemical treatments

The water vapour sorption isotherms relative to the treated Agave fibres are presented in Fig. 9 and compared to the untreated fibre isotherm as reference. Table 4 gives the parameter values calculated for the Park's model selected to simulate these isotherms. These data show that the chemical treatments result in a more or less significant reduction of the water sorption in the fibres, in agreement with the fluorescent microscopy images presented in Fig. 5, indicating a decrease of the hydrophilic sites at the fibre surface. In addition, from previous data published by Bessadok et al. (2007) relative to Alfa fibres, it seems that the chemical treatment effects are stronger with Agave than with Alfa fibres, certainly due to the higher density (lower porosity) of Alfa compared to Agave.

Among the four tested reagents, maleic anhydride (AM) seems to be the least efficient. This is certainly due to the substitution of ( $-\text{OH}$ ) groups for ( $-\text{O}-\text{CO}-\text{CH}=\text{COOH}$ ) groups which reduces only slightly the hydrophilic character of the fibres. Up until a water activity of 0.8, the untreated and treated fibres show practically the same isotherm; this corresponds to very close values of

the  $A_L$  and  $K_H$  (Park) parameters. For higher activities than 0.8, the tendency to form aggregates, according to Park ( $K_a$  and  $n$  values), would be slightly affected.

The treatments by acetic anhydride (Ac), acrylic acid (AA) and styrene (S) seems to be more efficient so that water sorption is decreased for the full activity range. This implies that, from Park's interpretation, the parameters  $A_L$ ,  $K_H$  and  $K_a$  tend to decrease.

#### 4.3. Water vapour sorption kinetics

##### 4.3.1. Diffusion coefficient determination

This section concerns the dynamic aspect of water vapour sorption in the fibres with the purpose of determining the water diffusion coefficient  $D$  by analysing the fibre sample mass variation kinetics. In order to examine the experimental data, as mentioned above in Section 2.2, the fibres are treated as dense and homogeneous cylinders, with a radius  $r$  much smaller than the length.

Taking into account the heterogeneity of the sample of fibres in length and diameter, and considering that the water vapour sorption measurements refer to the mass of dry fibres and to the mass of sorbed water, the weight average radius  $\langle r_w \rangle$  (equal to 122  $\mu\text{m}$  for the untreated fibres, see Section 3.1 and Appendix A) was chosen for the calculation of  $D$  (see Table 1).

The diffusion coefficient can be determined by two methods applied one to the beginning and the other to the end of sorption.

As long as the sorption uptake  $Q_t$  is inferior to 0.2,  $D$  is specified as  $D_1$  and the mass increase, according to Eq. (5), is proportional to  $\sqrt{t}$ :

$$Q_t = a_1 \sqrt{t}, \text{ with } a_1 = \frac{5\sqrt{D_1}}{\sqrt{\pi} \langle r_w \rangle} \text{ and} \quad (13)$$

$$D_1 = a_1^2 \frac{\pi \langle r_w \rangle^2}{16} \quad (14)$$

When  $Q_t$  is superior to 0.7,  $D$  is specified as  $D_2$  and  $Q_t$  is given, in agreement with Eq. (6), by the relation:

$$\ln(1 - Q_t) = a_2 t + b_2, \text{ with } a_2 = -\alpha_1^2 D_2 / \langle r_w \rangle^2 \text{ and} \quad (15)$$

$$D_2 = a_2^2 \langle r_w \rangle^2 / \alpha_1^2, \text{ with } \alpha_1 = 2.40483 \quad (16)$$

Fig. 10 gives an example of experimental data recorded during a sorption stage. In this example the water activity, initially equal to 0.27, is stabilized after one or two minutes at the value 0.34

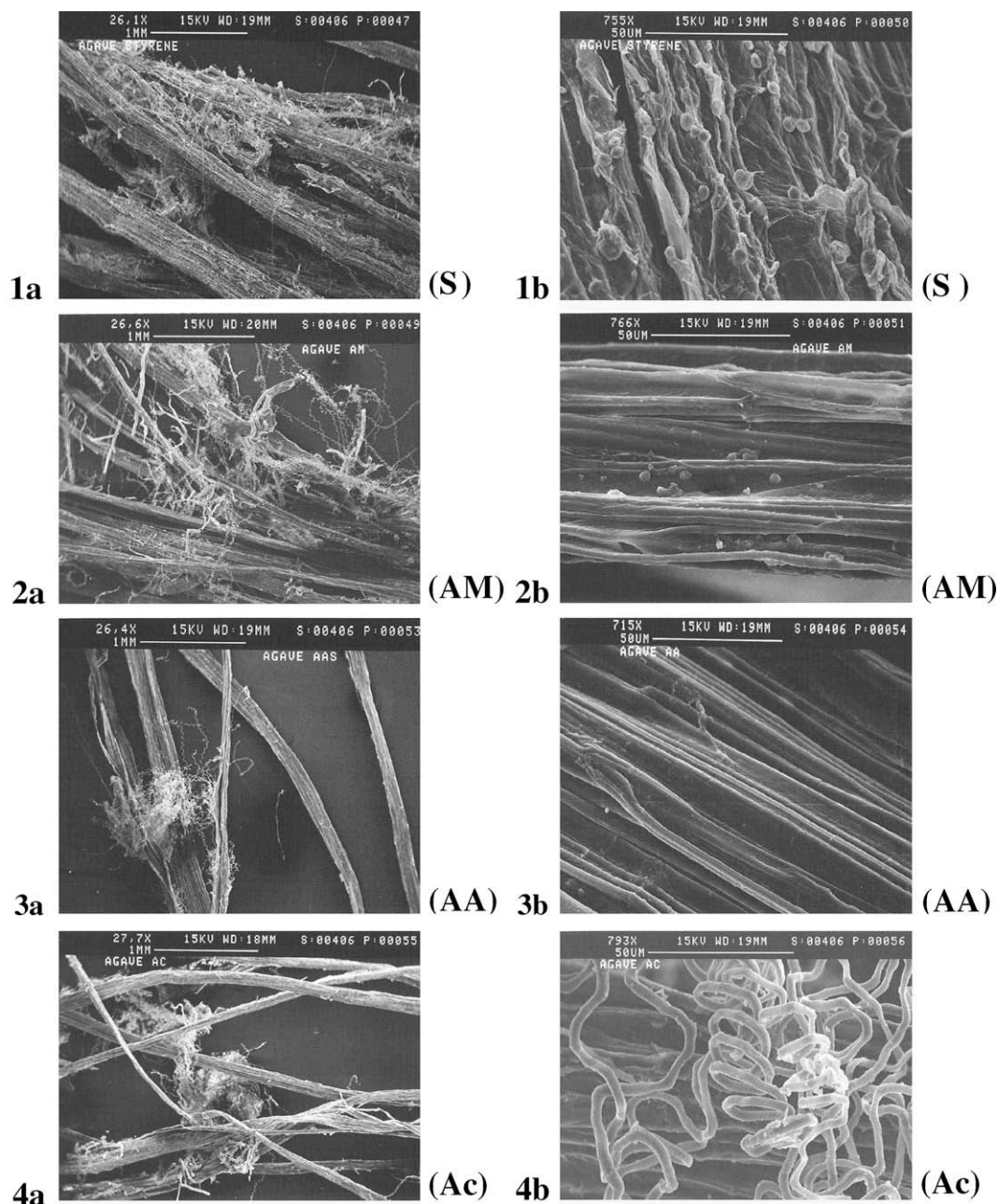


Fig. 6. SEM images of 1 (S), 2 (AM), 3 (AA) and 4 (Ac) treated Agave fibres. Series (a) for magnification  $\approx 27$  and series (b) for magnification  $\approx 755$ .

( $\Delta a_w = 0.07$ ). From a theoretical point of view, the zero time of kinetics is defined as the moment when the water vapour activity increases instantaneously by the increment  $\Delta a_w$ . For practical and technical purposes this increment occurs over about hundred seconds and during this period the boundary conditions of the system are not well defined.

The duration of the activity transition influences principally the beginning of the sorption and its effect vanishes progressively over time. To take this into account, a time lag  $t_d$  is introduced so that Eq. (13) can be written in the form:

$$Q_{t,\text{corr}}^2 = a_1^2(t - t_d) \quad (17)$$

where  $t_d$  obtained by linear extrapolation of  $Q_{t,\text{corr}}^2 = f(t)$  at the beginning of the sorption.

The values of  $D_1$  and  $D_2$  calculated for diffusion of water in the untreated Agave fibres are presented in Table 5. It appears that  $D_1$

and  $D_2$  depend appreciably on the water activity. This is visualized in Fig. 11 with the variations of  $D_1$  and  $D_2$  as a function of  $a_w$  in the semi-logarithmic scale  $\log(D) = f(a_w)$ . It can be observed, as a function of the water activity, first an increase of  $D_1$  and  $D_2$  then a decrease. This is indicative of a water sorption mechanism complying with the model of Park: a part of the water is adsorbed on specific sites (low mobility of the fixed water molecules) and the rest dissolved according to Henry's process (higher mobility of the dissolved molecules) later forming aggregates at high water activity (low mobility of the aggregates).

However other effects have to be considered. The sorption kinetics has been studied according to successive steps with limited activity increments  $\Delta a_w$  and, for each step, the value of  $D_2$  is found to be clearly larger (2–4 times) than  $D_1$ . This indicates heterogeneity of the fibres which could have a diffusion barrier at their surface. The  $D_2$  value (second half sorption) should be more representative of the dif-



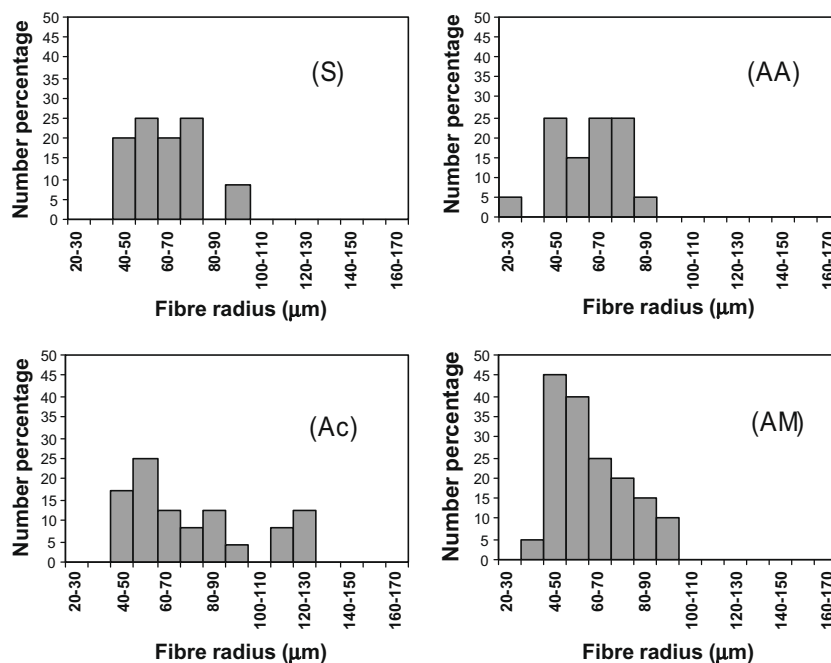


Fig. 7. Number radius distribution of (S), (AA), (Ac) and (AM) treated Agave fibres.

Table 1

Number-average radius  $\langle r_{nb} \rangle$  of untreated and treated Agave fibres.

Agave fibre	Number-average radius	$R^a$
Untreated fibre	109	1
(S) Treated	62	0.57
(AA) Treated	60	0.55
(Ac) Treated	79	0.72
(AM) Treated	67	0.61

<sup>a</sup>  $R$  = ratio (treated  $\langle r_{nb} \rangle$  / untreated  $\langle r_{nb} \rangle$ ).

Table 2

Water vapour sorption in untreated Agave fibres. Computed parameters of the Park's model, calculated for a water activity ranged from 0.1 to 0.9.

Park's model						
Parameters	$n$	$A_L$	$K_H$	$K_a$	Water activity range	$E$ (%) <sup>a</sup>
Untreated Agave fibre	8.4 <sup>c</sup>	0.015 <sup>b</sup>	0.16 <sup>b</sup>	0.47 <sup>c</sup>	0.1 <sup>d</sup> –0.9	2.1

$A_L$ ,  $K_H$  and  $K_a$  in g water/g dry fibre.

<sup>a</sup> Average deviation modulus in the indicated water activity range.

<sup>b</sup> Linear regression from Eq. (9) in the activity range  $0.1 \leq a \leq 0.5$ .

<sup>c</sup> Linear regression from Eq. (10) in the activity range  $0.5 \leq a \leq 0.9$ .

<sup>d</sup> The specific sorption sites of Langmuir are supposed to be saturated at this activity.

Table 3

Parameters of the Park's model simulating water vapour sorption in three vegetable fibres.

Fibre	Agave <sup>a</sup>	Alfa <sup>b</sup>	Flax <sup>c</sup>
$A_L$	0.015	0.013	0.021
$B_L$	(>50)	(>50)	47
$K_H$	0.016	0.012	0.011
$K_a$	0.47	0.61	0.25
$n$	8.4	10	18

$A_L$ ,  $K_H$  and  $K_a$  in g water/g dry fibre.

<sup>a</sup> This paper.

<sup>b</sup> Bessadok et al. (2007).

<sup>c</sup> Gouanvé et al. (2006).

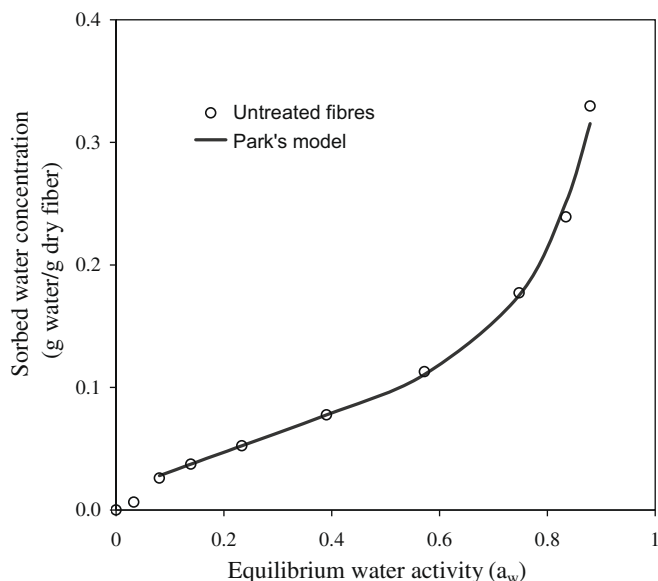


Fig. 8. Equilibrium water vapour sorption isotherm for untreated Agave fibres at 25 °C. Experimental points and curve calculated from Park's model (Eq. (3)) in the activity range  $0.1 < a_w < 0.9$ .

fusion of water in the core of the fibre while  $D_1$  (first half sorption) should be more characteristic of the diffusion through the surface.

#### 4.3.2. Effects of the chemical treatments on the sorption kinetics

The decrease of the fibre diameters, as well as the effect on water sorption isotherms, caused by the chemical treatments applied to Agave was described above (Sections 4.1.3 and 4.2.3). In order to estimate the impact of the resulting structural changes on the water diffusivity, it is convenient to exploit the sorption kinetics by using the appropriate weight average radius  $\langle r_w \rangle$ . In this purpose the data of Table 1 can be used assuming that the ratio

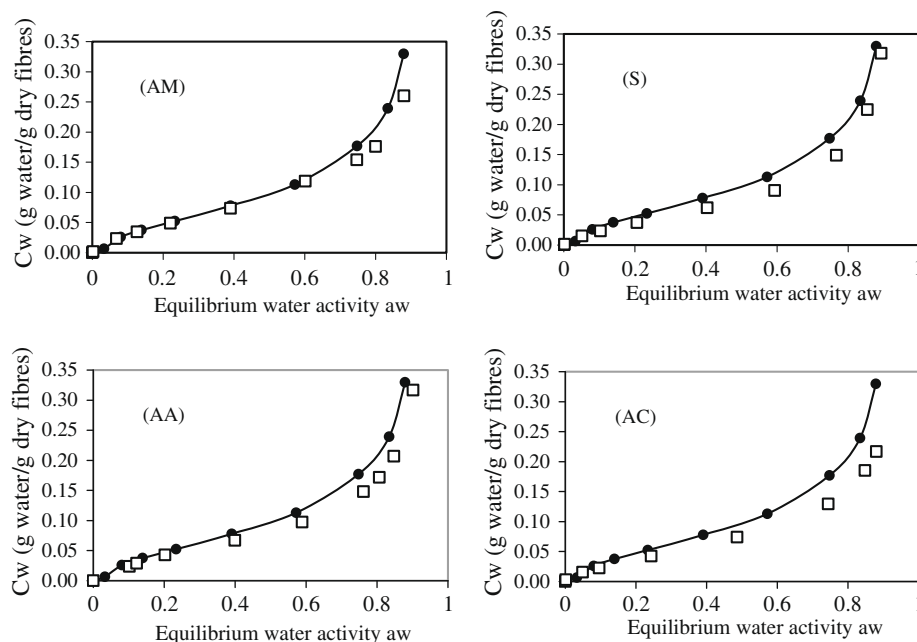


Fig. 9. Water vapour sorption at 25 °C. Sorption isotherms in untreated (full black circles) and (AM), (Ac), (AA) and (S) treated Agave fibres (open squares).

Table 4

Calculated parameters for the Park's model applied to the water vapour sorption in (AM), (Ac), (AA) and (S) treated Agave fibres.

Model	Park			
Water activity range	$0.1 \leq a \leq 0.9$			
Constant	$A_L$	$K_H$	$K_a$	$n$
Untreated	0.015	0.16	0.47	8.4
(AM) Treated	0.016	0.15	0.33	8.7
(Ac) Treated	0.010	0.13	0.26	8.3
(AA) Treated	0.017	0.13	0.47	9.9
(S) Treated	0.011	0.13	0.56	10.0

$A_L$ ,  $K_H$  and  $K_a$  in g water/g dry fibre.

Table 5

Computed diffusion coefficient  $D_1$  (first half sorption) and  $D_2$  (second half sorption) of water in untreated Agave fibres as a function of the equilibrium water activity  $a_w$ .

$a_w^a$	$D_1$ ( $m^2 s^{-1}$ )	$D_2$ ( $m^2 s^{-1}$ )
0.15	3.72 E-09	8.65 E-09
0.23	5.11 E-09	1.61 E-08
0.40	7.10 E-09	2.53 E-08
0.57	7.27 E-09	3.39 E-08
0.75	4.55 E-09	2.24 E-08
0.84	2.86 E-09	1.60 E-08
0.87	7.64 E-10	2.51 E-09

<sup>a</sup> Equilibrium water activity.

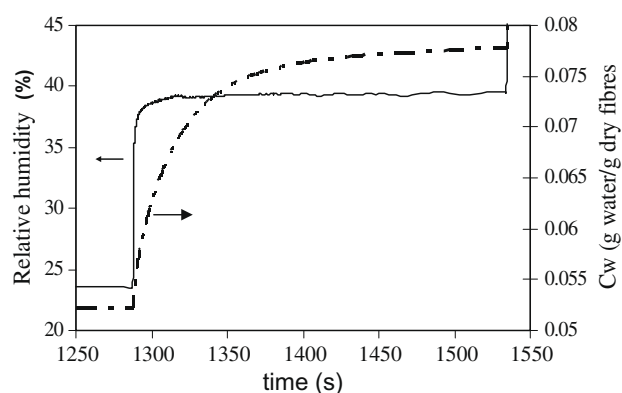


Fig. 10. Example of water vapour sorption in untreated Agave fibres at 25 °C. (a) Water uptake (g of water/g of dry fibres) vs. time (s); (b) water activity increment, relative humidity (%) in the sweeping nitrogen vs. time (s).

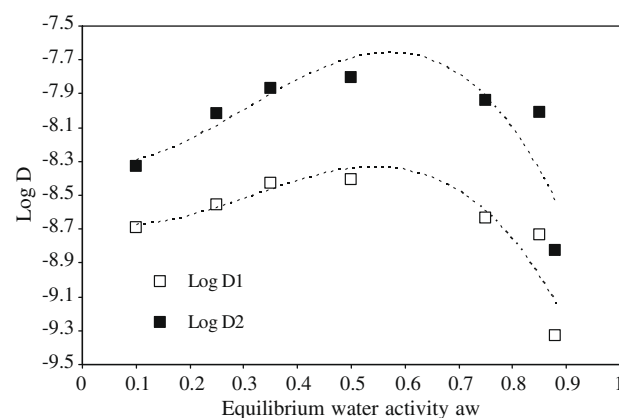


Fig. 11. Water vapour sorption in untreated Agave fibres at 25 °C. Evolution of the diffusion coefficients  $D_1$  and  $D_2$  as a function of the equilibrium water activity.

$R = \text{treated } \langle r_{nb} \rangle / \text{untreated } \langle r_{nb} \rangle$  remains unchanged when the weight average radius  $\langle r_w \rangle$  is used.

As in Fig. 11, Fig. 12 represents, for the untreated and (AM), (Ac), (AA) and (S) treated fibres, the evolution of the calculated diffusion coefficients  $D_1$  and  $D_2$  as a function of water activity, in a semi-logarithmic scale [ $\log(D) = f(a_w)$ ]. As a rule, for both  $D_1$  and  $D_2$ , it is ob-

served that the water diffusivity is decreased after treatment. This may be indicative of a local (superficial) increase of the fibre density caused by the treatment or of the additional barrier effect due to the binding of the chemical groups provided by (AM), (Ac), (AA) and (S) reagents.

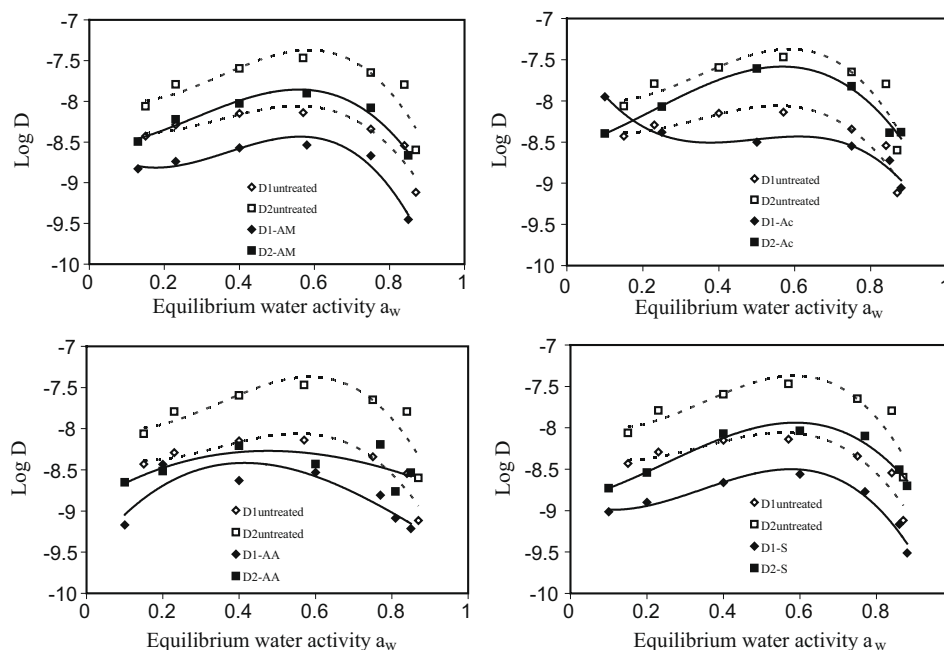


Fig. 12. Water vapour sorption at 25 °C in untreated and (AM), (Ac), (AA) and (S) treated Agave fibres. Evolution of  $D_1$  and  $D_2$  as a function of the water vapour activity.

## 5. Conclusion

The main purpose of this work was to chemically modify and characterize Agave fibres in order to improve their behaviour in humid environments before blending in a polymer matrix to make composites.

Agave fibres were extracted by a biological process, using pectinase, from plants coming from the Tunisian flora. The chemical treatment of the fibres was then achieved by using maleic anhydride (MA), acetic anhydride (Ac), acrylic acid (AA) and styrene (S) as reagents. The treated and untreated fibres were then characterized by using various physico-chemical methods like IRFT spectrometry, SEM and fluorescent microscopy and water sorption measurements by microgravimetry.

The IR spectra show, at the surface of the fibres, the formation of ester groups after (MA), (Ac) and (AA) treatments and the grafting of styrene after (S) treatment. The SEM images show some fibre morphology modifications caused by the treatments, in particular a decrease of the average radius of the fibres, while fluorescent microscopy highlights the changes of the hydrophilic character of the fibre surfaces.

Water vapor sorption isotherms of untreated and treated Agave fibres have been carried out at 25 °C. All the isotherms have a sigmoid or S-shape and correspond to type IV of the sorption in polymers Rogers classification. This can be accurately simulated by two families of models. In the first (BET and GAB) the water molecules are adsorbed in several layers, in the second (Park) a part of water is adsorbed on hydrophilic Langmuir sites while the other part is dissolved according to Henry's law then forms aggregates at high activity. Considering our experimental results, the Park's model was found to be the more appropriate with respect to its accuracy and the extent of its domain of validity.

The (Ac), (AA) and (S) treatments have as a common effect to noticeably decrease the water sorption in Agave fibres in the whole water activity range, which is favorable in the purpose of composite polymer materials. This effect has been partly attributed to the disappearance of a fraction of the hydrophilic sites at the fibre surface, and perhaps at depth, as a result of the treatments.

In addition, analysis of the water sorption kinetics of untreated and treated agave fibres indicates that (i) water is probably more mobile in the core than at the surface of the fibres, (ii) the variation of the water diffusion coefficient vs. water activity complies with the Park's model hypothesis, (iii) the global diffusivity of water is clearly decreased, in pretty much the same proportion, by the different chemical treatments.

In conclusion surface analysis of the fibres and water vapour sorption measurements give significant informations about the effects of the chemical treatments, from the structural point of view and mainly about the fibre behaviour in humid environments. Globally, the (Ac), (AA) and (S) treatments lead to similar results, improving the agave fibre properties in view of composite applications.

Finally, to have a better assessment of the water sorption in agave fibres, it will be interesting to consider not only the presence of residual water molecules in the dry mass (for isotherms) but also the porosity of the fibres (lumen) associated to the dimension changes during the sorption process (for the determination of the diffusion coefficients).

## Acknowledgements

The authors thank «ICF», «Institut de Coopération Français de l'ambassade de France en Tunisie» and the «Ministère de l'Enseignement Supérieur Tunisien» for their financial supports.

## Appendix A

### A.1. Mass average radius of the fibres

In a sample, the fibre population can be stated by a number fraction:

$$X_{i,nb}\% = n_i / \sum_{i=1}^N n_i \times 100 \quad (\text{A.1})$$

where  $n_i$  is the number of fibres in the  $i$ th interval  $[r_i, r_i + \Delta r]$  and  $N$  is the number of intervals.

And a number-average fibre radius:

$$\langle r_{nb} \rangle = \frac{\sum_{i=1}^N r_{i,m} n_i}{\sum_{i=1}^N n_i} \quad (\text{A.2})$$

where  $r_{i,m} = r_i + \Delta r/2$  is an average value of  $r$  in the interval  $[r_i, r_i + \Delta r]$ .

Considering that the water vapour sorption measurements refer to the mass of sorbent (mass of fibres) and sorbate (water), it is more convenient to express a weight fraction:

$$X_{i,w} \% = m_i / \sum_{i=1}^N m_i \times 100 \quad (\text{A.3})$$

with  $m_i = n_i \pi r_{i,m}^2 \rho h_i$  where  $m_i$  is the total mass of fibres in the  $i$ th interval,  $\rho$  is the fibre volumic mass and  $h_i$  is the average fibre length in the  $i$ th interval.

And a weight average radius:

$$\langle r_w \rangle = \frac{\sum_{i=1}^N n_i r_{i,m}^3 h_i}{\sum_{i=1}^N n_i r_{i,m}^2 h_i} \quad (\text{A.4})$$

## References

- Abdelmoula, S., Mzid, K., El Achari, A., Mhenni, F., Rammah, M. E., & Caze, C. (1997). Modification of nylon and polyesters via graft copolymerization. *Journal of Macromolecular Science, Reviews in Macromolecular Chemistry and Physics*, C37(4), 649–686.
- Ahrens, F. W., Gulya, T., Worry, G. L., Walter, W. P. (1998). Papermaking fabric, process for producing high bulk products and the products produced thereby. US Patent, 5, 574–853.
- Angot, A. (1965). *Compléments de mathématiques* (5th ed.). Paris: Collection Technique et Scientifique du C.E.N.T..
- Anon, I. (1974). Algeria goal of self-sufficiency being realized. *Pulp Paper International*, 16(10), 7.
- Aranberri-Askargorta, I., Lampcke, T., & Bismarck, A. (2003). Wetting behavior of flax fibers as reinforcement for polypropylene. *Journal of Colloid and Interface Science*, 263, 580–589.
- Atchison, J. E., Mc Govern, J. N., Kocurek, M. J., & Steven, F. (1983). Non-wood plant as raw material for pulp and paper. *Tappi*, 1, 154–163.
- Bellamy, L. J. (1975). *The infra-red spectra of complex molecules* (3rd ed.). London: Chapman and Hall Ltd.
- Bessadok, A., Marais, S., Gouanvé, F., Colasse, L., Zimmerlin, I., Roudesli, S., et al. (2007). Effect of chemical treatments of Alfa (*Stipa tenacissima*) fibers on water-sorption properties. *Composite Science & Technology*, 67, 685–697.
- Bledzki, A. K., & Gassan, J. (1999). Composites reinforced with cellulose based fibres. *Progress in Polymer Science*, 24, 221–274.
- Brunauer, S., Emmett, P. H., & Teller, E. (1938). Adsorption of gases in multimolecular layers. *Journal of the American Chemical Society*, 60, 309–319.
- Cantero, G., Arbelaiz, A. K., Llano-Ponte, R., & Mondragon, I. (2003). Effects of fibre treatment on wettability and mechanical behaviour of flax/polypropylene composites. *Composite Science & Technology*, 63, 1247–1254.
- Crank, J., & Park, G. S. (1968). In *Diffusion in polymers*. London and New-York: Academic Press.
- Crank, J. (1975). *The mathematics of diffusion* (2nd ed.). Oxford University Press.
- Cruz, R. A., Mendoza, A. M., Calado-Vieira, M., & Heinze, T. (1999). Studies on grafting of cellulosic materials isolated from Agave lechuguilla and fourcroydes. *Die Angewandte Makromolekulare Chemie*, 273, 86.
- Detallante, V., Langevin, D., Chappey, C., Métayer, M., Mercier, R., & Pineri, M. (2002). Kinetics of water vapour sorption in sulfonated polyimide membranes. *Desalination*, 148, 333–339.
- Garside, P., & Wyeth, P. (2003). Identification of cellulosic fibres by FTIR spectroscopy. I: Thread and single fibre analysis by attenuated total reflectance. *Studies in Conservation*, 48, 269–275.
- Gouanvé, F., Marais, S., Morvan, C., Métayer, M., Poncin-Epaillard, F. (2006). Composites polyesters insaturés renforcés par des fibres de lin. Effets de traitements plasma froid et autoclave sur les propriétés perméométriques. RCM-16, Composites à fibres végétales, Hermès Sciences, ISBN 2-7462-1430-X, 115–128.
- Grunert, M., Winter, W.T. (2000). Paper in 2nd annual partnerships for environmental improvement and economic development conference, wood and cellulose: Building blocks for fuels and advanced materials. Syracuse, N.Y., USA.
- Guggenheim, E. A. (1966). *Application of Statistical Mechanics* (Ch. 11). Clarendon Press.
- Iglesias, H. A., & Chirife, J. L. (1975). Water sorption isotherms in sugar beet root. *Journal of Food Technology*, 10, 299–308.
- Iniguez-Covarrubias, G., Diaz-Teres, R., Sanjuan-Duenas, R., Anzaldo-Hernandez, J., & Rowell, R. M. (2001). Utilization of by-products from the tequila industry. Part 2: Potential value of Agave tequilana Weber azul leaves. *Bioresource Technology*, 77, 101–111.
- Jonquière, A., & Fane, A. (1998). Modified BET models for modeling water vapor sorption in hydrophilic glassy polymers and systems deviating strongly from ideality. *Journal of Applied Polymer Science*, 67, 1415–1430.
- Joseph, K., Thomas, S., & Pavithran, C. (1995). Effect of ageing on the physical and mechanical properties of sisal-fiber-reinforced polyethylene composites. *Composite Science & Technology*, 53(1), 99–110.
- Khalil, H. P. S. A., & Rozman, H. D. (2000). Rice husk-polyester composites: The effect of chemical modification of rice husk on the mechanical and dimensional stability properties. *Polymer Plastic & Technology Engineering*, 39, 757–781.
- Khalil, H. P. S. A., Ismail, I., Rozman, H. D., & Ahmad, M. N. (2001). The effect of acetylation on interfacial shear strength between plant fibres and various matrices. *European Polymer Journal*, 37, 1037–1045.
- Kohler, R., Dueck, R., Ausperger, B., & Alex, R. (2003). A numeric model for the kinetics of water vapor sorption on cellulosic reinforcement fibers. *Composite Interfaces*, 10(2/3), 255–276.
- Kreze, T., Iskrac, S., Sliligoj-Smole, M., Stana-Kleinscheck, M., Strnad, S., & Fakin, D. (2005). Flax fibers sorption properties influenced by different pre-treatment processes. *Journal of Natural Fibres*, 2(3), 25–37.
- Leung, H. K. (1983). Water activity and other colligative properties of foods. In *ASAE annual meeting*, Chicago, Paper no 83.
- Mali, S., Sakanaka, L. S., Yamashita, F., & Grossmann, M. V. E. (2005). Water sorption and mechanical properties of cassava starch films and their relation to plasticizing effect. *Carbohydrate Polymers*, 60, 283–289.
- Morton, W. E., & Hearle, J. W. S. (1997). *Physical properties of textile fibers*. UK: The Textile Institute.
- Okubayashi, S., Grissier, U. J., & Betchold, T. (2004). A kinetic study of moisture and desorption on lyocell fibers. *Carbohydrate Polymers*, 58, 293–299.
- Olson, A. M., & Salmén, L. (2004). The association of water to cellulose and hemicellulose in paper examined by FTIR spectroscopy. *Carbohydrate Research*, 339, 813–820.
- Park, G. S. (1986). Transport principles: Solution, diffusion and permeation in polymer membranes. In P. M. Bungay et al. (Eds.). *Synthetic membranes: Science, engineering and applications* (57). Holland: Reidel Pub..
- Ricks, M., Vogel, R., Elston, P. S., & Hivnor, C. (1999). Purpuric agave dermatitis. *Journal of the American Academy of Dermatology*, 40, 356–358.
- Rogers, C. E. (1965). Solubility and diffusivity. In D. Fox, M. M. Labes, & A. Weissberger (Eds.), *Physics and Chemistry of the organic solid state* 2. Interscience Pub..
- Rong, M. Z., Zang, M. Q., Liu, Y., Yang, G. C., & Zeng, H. M. (2001). The effect of fiber treatment on the mechanical properties of unidirectional sisal-reinforced epoxy composites. *Composite Science & Technology*, 61, 1437–1447.
- Sreekala, M. S., & Thomas, S. (2003). Effect of fibre surface modification on water-sorption characteristics of oil palm fibres. *Composite Science & Technology*, 63, 861–869.
- Thykeson, M., Sjöberg, L. A., & Ahlgren, P. (1997). Making paper from Montana's straw. *Nordic Pulp Paper Research Journal*, 12, 128–134.
- Toribio, F., Bellat, J. P., Nguyen, P. H., & Dupont, M. (2004). Adsorption of water vapor by poly(styrenesulfonic acid) sodium salt. Isothermal and isobaric adsorption equilibria. *Journal of Colloid and Interface Science*, 280, 315–321.
- Tronc, E., Hernandez-Escobar, C. A., Ibarra-Gomez, R., Estrada-Monje, A., Navarrete-Bolanos, J., & Zaragoza-Contreras, E. A. (2007). Blue agave fiber esterification for the reinforcement of thermoplastic composites. *Carbohydrate Polymers*, 67, 245–255.